A supplement to "Synoptic-scale meteorological control on reactive bromine production and ozone depletion in the Arctic boundary layer: 3-D simulation with the GEM-AQ model" by K. Toyota et al.

K. Toyota[1,2], J. C. McConnell[1], A. Lupu[1], L. Neary[1,†], C. A. McLinden[2], A. Richter[3], R. Kwok[4], K. Semeniuk[1], J. W. Kaminski[1], S.-L. Gong[2], J. Jarosz[1], M. Chipperfield[5], and C. E. Sioris[2]

[1]Department of Earth and Space Science and Engineering, York University, Toronto, Ontario, Canada
[2]Air Quality Research Division, Science and Technology Branch, Environment Canada, Toronto, Ontario, Canada
[3]Institute of Environmental Physics, University of Bremen, Bremen, Germany
[4]Jet Propulsion Laboratory, California Institute of Technology, Pasadena, California, USA
[5]School of Earth and Environment, University of Leeds, Leeds, UK
[†]Now at Belgian Institute for Space Aeronomy (BIRA-IASB), Brussels, Belgium

October 2, 2010

S1 Surface winds and temperatures simulated by GEM

Simulated surface winds and temperatures are evaluated by using routine and research observational data obtained at the ground level across the Arctic (red stars in Fig. 2 of the main paper), available electronically from several sources including National Climatic Data Center (NCDC, http://www.ncdc.noaa.gov/) for routine observations maintained by various national bureaus, NOAA/ESRL Global Monitoring Division (http://www.esrl.noaa.gov/gmd/) for data from Barrow, Alaska, Norwegian Institute for Air Research (http://www.nilu.no/niluweb/services/zeppelin/) for data from Zeppelin, Svalbard, Norway, Environment Canada (http://www.msc-smc.ec.gc.ca/natchem/) for data from the Alert GAW station, Ellesmere Island, Canada (Environment Canada, 2001), and National Snow and Ice Data Center (http://nsidc.org/) for data from the J-CAD 3 buoy drifting near the North Pole during our simulation period (Takizawa and Kikuchi, 2004). Nominally all of these meteorological data are hourly archives, but actually more than half of the NCDC data used here are 6-hourly. Statistical metrics of comparison between the model and observations from all the sites are summarized in Table S1.

Temporal variations in wind speed and direction are simulated reasonably well at sites located within smooth topography, including Barrow, Resolute, Inuvik, Ostrov Kotelnyj, Ostrov Golomjannyj and the J-CAD 3 buoy (see Figs. S1c-d,f and correlation coefficients between the model and the observations in Table S1). This indicates that boundary-layer meteorology at these sites was largely under the control of synoptic- and/or planetary-scale forcing resolved at the grid resolution employed for the present simulation.

Correspondence to: K. Toyota (Kenjiro.Toyota@ec.gc.ca)

For instance, Fig. 8a of the main paper shows surface air temperatures and wind vectors simulated at 12 UTC for each day between 15-22 April 2001. During this period, major disturbances in the Arctic surface meteorology apparently had length scales greater than 1000 km, emerging, migrating and/or vanishing of which can be tracked well at daily interval. Strong surface winds, which often accompany increased surface air temperatures, were induced by the bipolar development of high and low pressure systems seen in the 850 hPa height fields (Fig. S2a). The 500 hPa height fields developed the same horizontal structures largely in phase with the 850 hPa height fields (Fig. S2b), indicating a formation of blocking highs and lows as a major cause of large-scale disturbances during this period (Pelly and Hoskins, 2003; Croci-Maspoli et al., 2007; Tyrlis and Hoskins, 2008a,b).

Polar lows also create major disturbances to surface meteorology in the Arctic. They are intense maritime mesocyclones formed over the Arctic and sub-arctic open ocean when a colder air mass is advected from over land or over the ice-covered ocean (Rasmussen and Turner, 2003). But the climatology of their migration to the ice-covered Arctic Ocean is poorly understood because of limited in-situ observations and a difficulty in cloud classification over the sea ice from meteorological satellites (e.g., Serreze and Barry, 1988; Blechschmidt, 2008). Considering their short-lived nature and typical spatial scales of 200-1000 km, we should not expect a lot of chances for simulating polar lows successfully at the present grid resolution ($\approx 100\,\mathrm{km} \times 100\,\mathrm{km}$). There was one episode, however, during 6-7 April 2001 when a intense, closed vortex migrated from the south through Bering Strait and is also reproduced reasonably well by the model (Figs. S3a-b). The vortex had weakened by the time it approached Barrow on 8 April, but a warm advection from the south associated with this weather system led to an increase

Table S1. Statistical metrics of comparison between observed and simulated hourly surface air temperatures and winds at selected Arctic sites[a] during April 2001: Vector correlation coefficients between observed and simulated surface winds (r_V)[b], scalar correlation coefficients between observed and simulated surface wind speeds (r_S), number of samples (n), mean and standard deviation values of observed surface wind speed (S_{obs}), mean bias (B_S) and root mean squared error (E_S) of simulated surface wind speed, correlation coefficients between observed and simulated surface air temperatures (r_T), mean and standard deviation values of observed surface air temperature (T_{obs}), and mean bias (B_T) and root mean squared error (E_T) of simulated surface air temperature.

	Wind statistics						Temperature statistics				
	r_V	r_S	n	S_{obs} [m/s]	B_S [m/s]	E_S [m/s]	r_T	n	T_{obs} [°C]	B_T [°C]	E_T [°C]
Alert CFS	0.58	0.44	174	3.1±3.3	+0.0	2.9	0.85	238	-25.6 ± 5.9	−0.5	3.2
Alert GAW	0.74	0.57	719	3.2±3.8	−0.3	3.2	0.86	720	-23.7 ± 6.4	−2.4	4.1
Barrow	1.20	0.83	646	5.6±3.1	+0.5	2.1	0.87	665	-16.9 ± 4.7	−1.3	2.9
Eureka	0.57	0.32	466	3.2±3.2	−0.1	3.0	0.90	651	-25.3 ± 7.0	+0.5	3.1
Hall Land	0.80	0.44	194	4.2±2.9	+1.0	3.2	n.a.	0	n.a.	n.a.	n.a.
Inuvik	0.92	0.50	674	3.1±1.5	+0.2	1.6	0.85	714	-11.2 ± 6.5	−3.2	4.7
Resolute	0.89	0.70	610	5.6±3.9	−1.3	3.1	0.80	705	-22.2 ± 4.7	−2.5	4.5
Golomjannyj	0.95	0.64	231	5.4±3.0	−0.9	2.5	0.79	232	-23.9 ± 4.4	−3.5	4.8
Kotelnyj	1.07	0.76	225	6.9±4.1	−1.3	3.1	0.92	232	-20.4 ± 5.3	−1.2	2.6
Vrangelja	0.92	0.43	150	4.4±3.6	+0.4	3.4	0.86	187	-15.7 ± 4.8	−3.0	3.9
Ny Ålesund	0.29	0.50	230	2.9±2.6	+2.2	3.6	0.94	234	-11.0 ± 7.1	+1.4	3.0
Zeppelin	0.66	0.50	650	2.7±1.9	+4.0	5.2	0.96	720	-12.4 ± 6.7	+0.1	1.9
J-CAD 3 buoy	0.97	0.65	447	3.0±1.5	+1.8	2.6	0.85	505	-21.8 ± 5.7	−2.3	5.0

Note: [a]The location of each station is indicated in Figs. 2a-b of the main paper; [b]Calculated according to Crosby et al. (1993), $-\sqrt{2}$ for perfect anti-correlation and $\sqrt{2}$ for perfect correlation.

in surface air temperature as large as 10 K at Barrow on 7 April (Fig. S1c).

On the other hand, the model at the present grid resolution does not perform as well for simulating surface winds near or within mountains, including Alert CFS/GAW stations, Eureka, Ny Ålesund, and Zeppelin (Table S1 and Fig. S1a,e).

For instance, downslope flows induced by a surface radiative cooling are known to prevail in a shallow layer over Greenland (e.g., Bromwich et al., 1996; Cassano et al., 2001) and also around Alert in the northeastern slope of Ellesmere Island (e.g., Hopper et al., 1998; Ola et al., 2007). The grid resolution of our model is apparently too coarse properly to resolve topography responsible for the formation of downslope flows observed at Alert (Ola et al., 2007, see Fig. 8). Note, however, that temporal variations in surface air temperature and wind speed/direction at Hall Land, Greenland, located across the channel from Alert (see Fig. 2b of the main paper) show some coherence with those observed at Alert (Figs. S1a-b). In addition, the coherent part of the temperature/wind variations observed at two Alert stations and Hall Land appears to be reproduced quite reasonably by the model. Thus, even though boundary-layer meteorology at Alert is influenced strongly by unresolved meso-scale flows, the model appears to do a reasonable job in simulating synoptic disturbances around the site.

Five cases of short-lived wind episodes observed at the Alert GAW station on 9, 11, 24, 25 and 28 April are the prominent examples of downslope flow, which is not simulated very well by our present model. During these episodes, wind speed at the Alert GAW station abruptly increased to 10-15 $\mathrm{m\ s^{-1}}$ and lasted only for several hours. The wind direction was southerly to southwesterly, typical of the downslope flow at Alert (Ola et al., 2007). Except for the case on 28 April when the surface wind speed similarly increased at Alert CFS, those windy episodes were not observed at Alert CFS and Hall Land, indicating limited horizontal and vertical scales of the events. Surface air temperature also increased by as high as 10 K during the events, probably because air had been transported from and/or mixed with a free-tropospheric air mass. This also explains the surface ozone increase concurrently observed at the Alert GAW station (Fig. 3a of the main paper). Maxwell (1980) reported foehn storms accompanying strong southwesterly winds with an increase in temperature at Alert sometimes by more than 20 K in a few hours during the winter.

On many occasions, simulated wind speeds at two stations, Ny Ålesund and Zeppelin, in Svalbard, Norway are too strong compared with observations (Table S1 and Fig. S1e). Unresolved topography may be one of the reasons, but these sites are also located near the boundary between the ice-covered and ice-free oceans so that spatial variations in heat supply to the atmosphere (as a driving force of polar lows and other meso-scale circulations) may not have been resolved very well at the present grid resolution.

Correlation coefficients between simulated and observed surface air temperatures generally exceed 0.8 (Table S1). Diurnal temperature variations play a role here, but variability at time scales longer than a day is also simulated reasonably

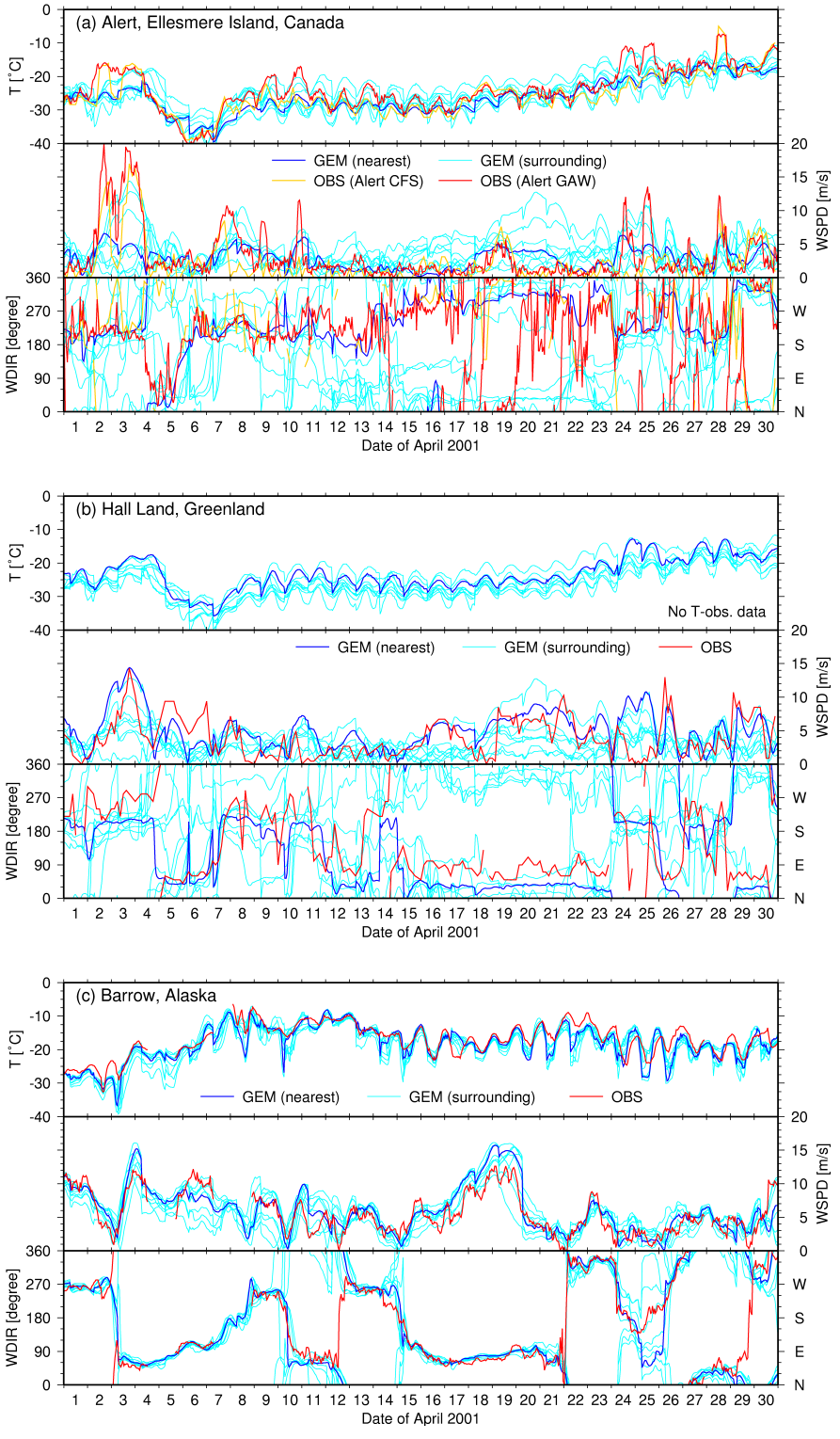

Fig. S1. Hourly surface air temperatures and wind speeds/directions observed at **(a)** Alert CFS (orange lines) and GAW (red lines) stations, Ellesmere Island, Canada, **(b)** Hall Land, Greenland, **(c)** Barrow NOAA/ESRL station, Alaska, **(d)** Ostrov Golomjannyj, Russia, **(e)** Zeppelin, Svalbard, Norway, and **(f)** the JAMSTEC Compact Arctic Drifter (J-CAD) 3 buoy drifting near the north pole, plotted along with those simulated by the GEM model at the nearest (blue lines) and 8 surrounding (light blue lines) grid cells. The simulated values are taken from the lowest model level, except for Zeppelin where the 4th lowest vertical model level (~ 470 m a.s.l.) is chosen to best match the altitude of the station.

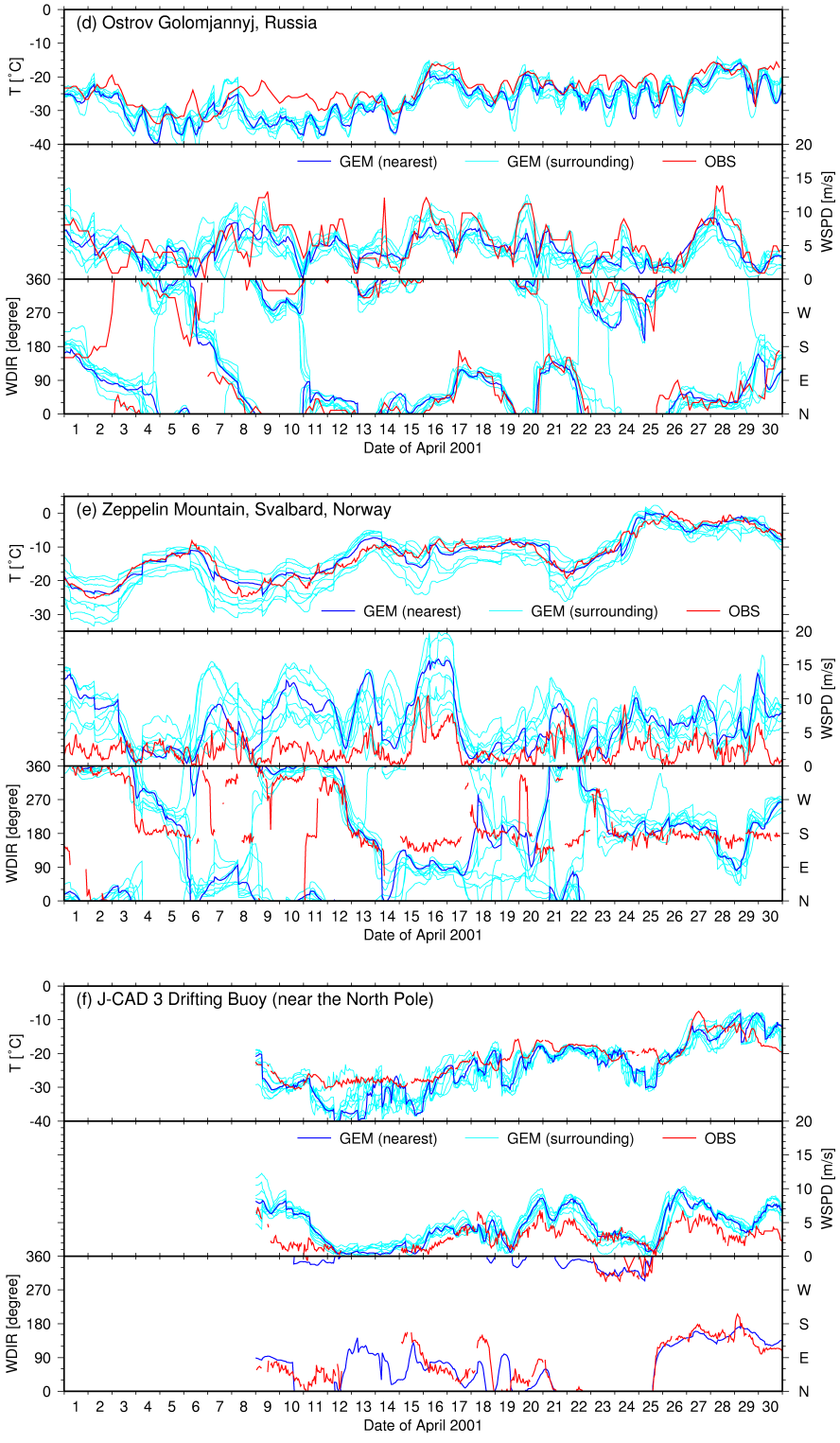

Fig. S1. (Continued.)

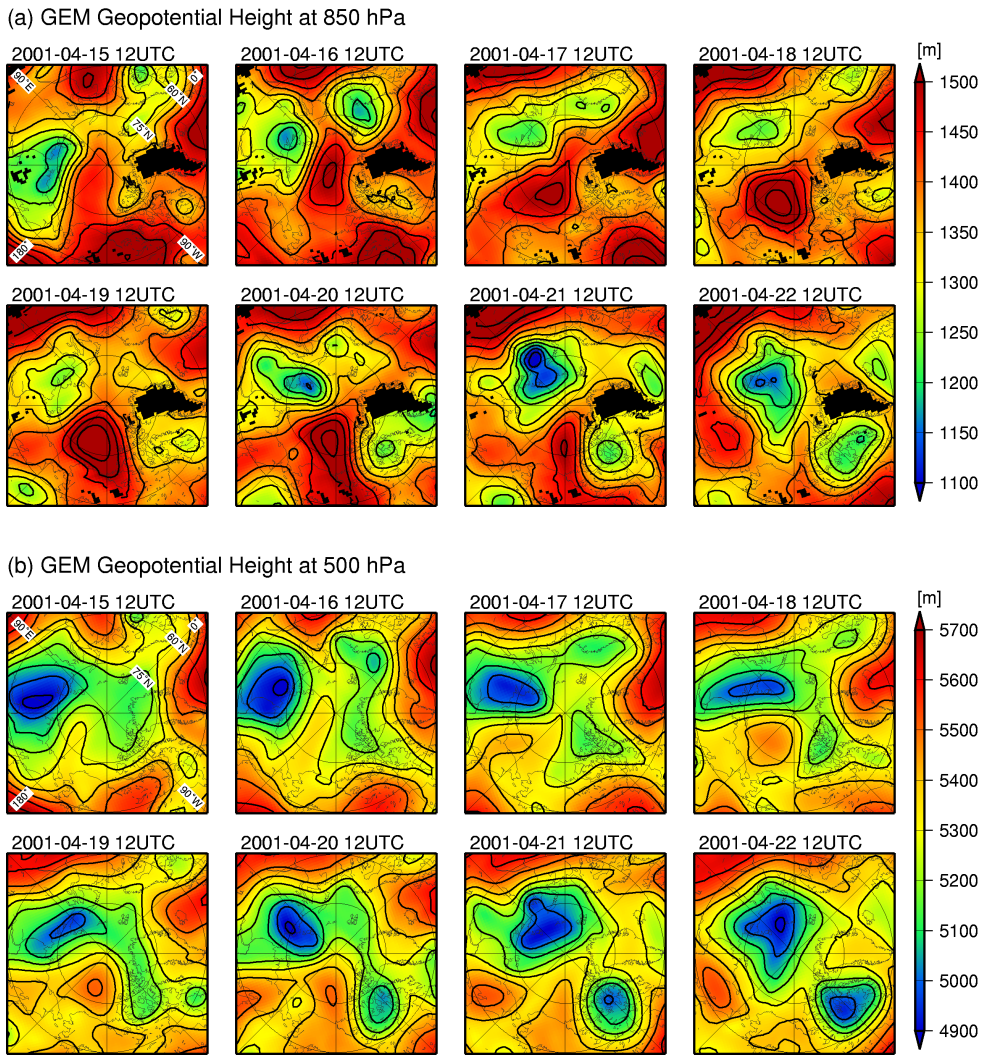

Fig. S2. (a) Geopotential height fields (contoured every 50 m) at 850 hPa level at 12 UTC for each day between 15-22 April 2001 simulated by the GEM model; and **(b)** The same as (a) but for geopotential height (contoured every 100 m) at 500 hPa level.

well at many sites (Figs. S1a-f), indicating again the capability of the model in simulating synoptic disturbances.

For most sites examined here, however, simulated surface air temperatures exhibit a cold bias by $-0.5\,\mathrm{K}$ to $-3.5\,\mathrm{K}$ in monthly mean against in-situ observations (Table S1). One may question the quality of the observational data, because automated meteorological observations are quite challenging in the cold, high-latitude environment owing to possible physical interferences to instruments such as a formation of frost and snowdrift. But there is some consistency for the occurrence of cold bias in simulated surface air temperatures. It appears that the model simulates an excessive radiative cooling at the surface and in the near-surface air during the night when the wind speed is low (Figs. S1c-d and f). Fortunately, as discussed in Sect. 3 of the main paper, bromine release from the snowpack is simulated to occur mainly when/where surface wind speed is high so that the issue of the cold bias here should not significantly undermine our discussion about the impacts of temperature on bromine release.

In the polar lower troposphere, air cooled rapidly under the clear sky is likely to promote a formation of 'diamond dust', by which the surface radiative cooling can be slowed down significantly from what would otherwise occur at a rate by more than $20\,\mathrm{K\ day^{-1}}$ (Curry, 1983; Curry and Ebert, 1992; Walsh and Chapman, 1998). It is a very intricate process and requires a cloud microphysics parameterization dedicated to simulating the diamond dust, which, to our knowledge, has not been implemented to operational weather forecast models. In general, the reliability of radiative transfer calculations for the polar atmosphere becomes rather questionable in the presence of clouds, because the parameterizations of cloud and precipitation processes are often extrapolated from

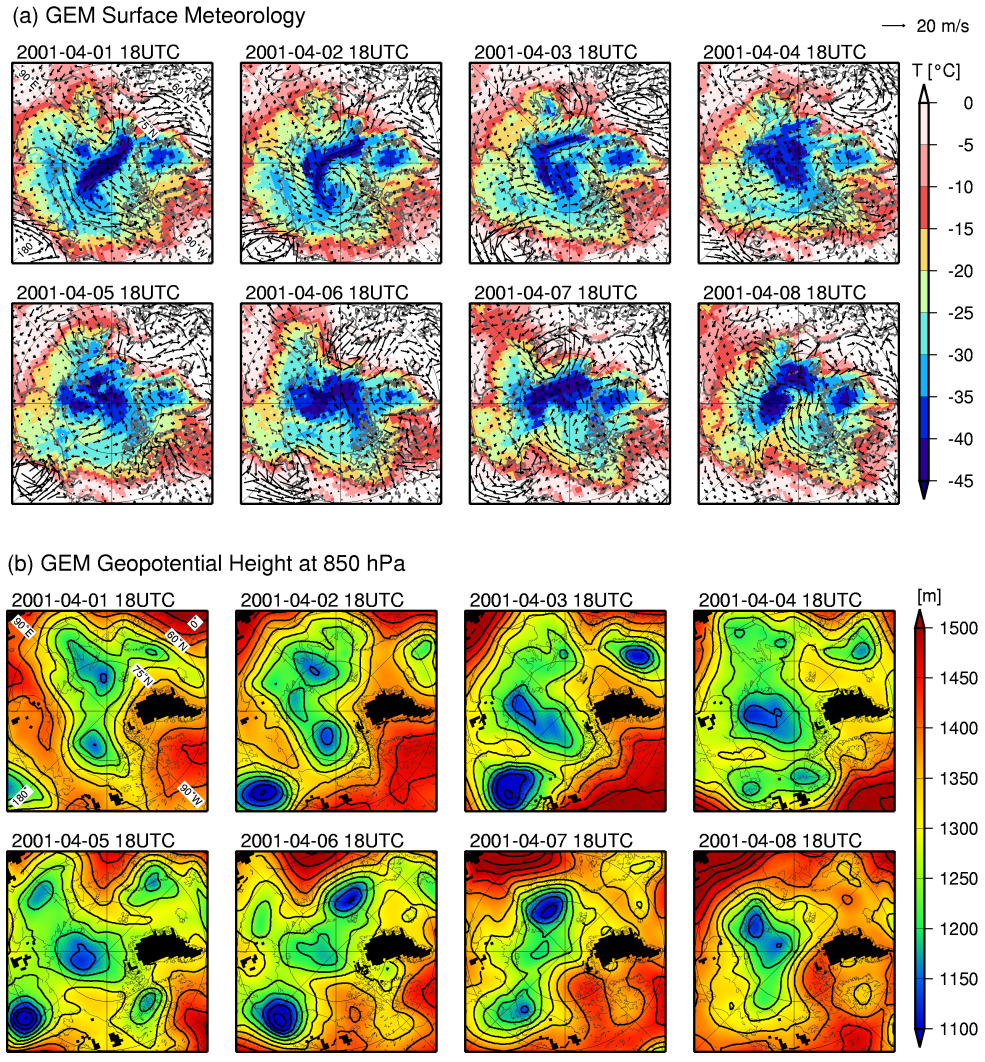

Fig. S3. **(a)** Surface air temperatures (color shade, in C) and wind vectors (arrow length for the wind speed of $20\,\mathrm{m\,s^{-1}}$ is indicated in the top right corner) at 18 UTC for each day between 1-8 April 2001 simulated by the GEM model; and **(b)** The same as (a) but for geopotential height fields (contoured every 50 m) at 850 hPa level.

what have been validated for cases observed at lower latitudes (e.g., Inoue et al., 2006).

It should be noted that the present meteorological simulation does not necessarily comply with most recent versions of GEM in use for operational forecast. Also, in a model inter-comparison study by Cuxart et al. (2006), the turbulent-diffusivity parameterization used in GEM was found to perform among the best in operational/research models tested for simulating scalar profiles in a stably stratified boundary layer typical of the Arctic. Simulated meteorology examined here could have been in a better agreement with observations by choosing a more sophisticated package for cloud physics and/or running the model at higher resolutions (e.g., Mailhot et al., 2002). The configuration and grid resolution of the present model are chosen so as to perform many model runs within a reasonable computational time while adjusting parameters related to air-snowpack chemical interactions.

S2 Ground-level aerosol concentrations simulated by GEM-AQ

It is beyond the scope of the present study to evaluate simulated aerosol concentrations in detail, but we briefly compared simulated sulfate and sea-salt aerosol concentrations with those observed (as non-sea-salt sulfate and sodium, respectively) at the ground level from three Arctic sites (Fig. S4).

For non-sea-salt sulfate, agreement between the model and the observations is generally within a factor two except at

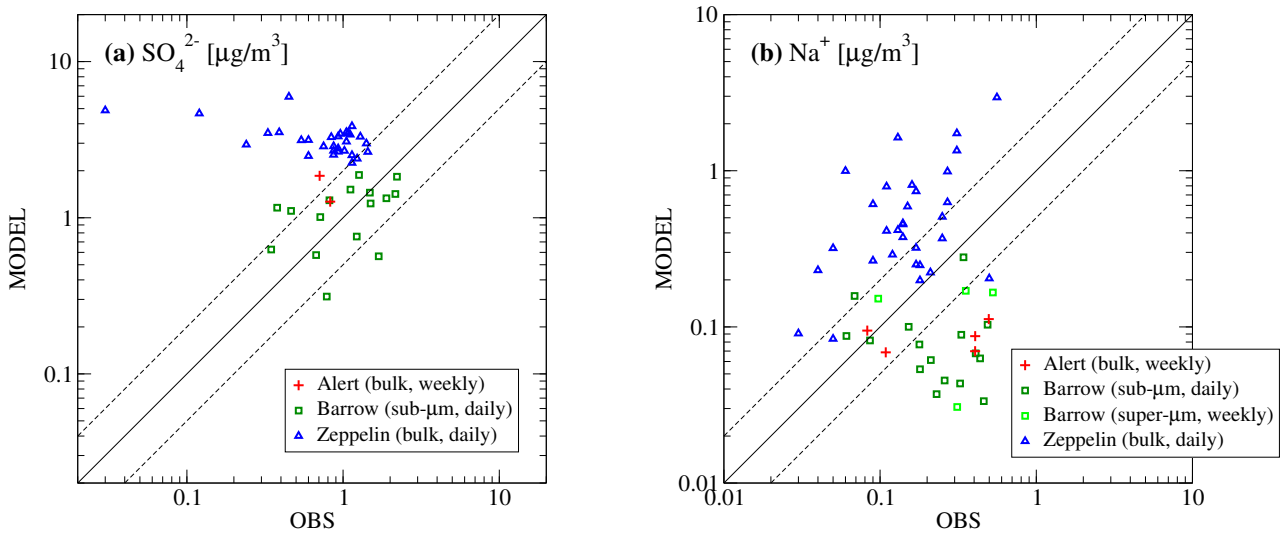

Fig. S4. Scatter plots of simulated non-sea-salt sulfate **(a)** and sodium **(b)** concentrations (from Run 3) versus those observed during April 2001 at the ground level from three Arctic stations (Quinn et al., 2007): Alert, Canada (electronic data available from the Canadian National Atmospheric Chemistry Database at http://www.msc.ec.gc.ca/natchem/); Barrow, Alaska (electronic data available from the Pacific Marine Environmental Laboratory, National Oceanic and Atmospheric Administration at http://saga.pmel.noaa.gov/data/); and Zeppelin, Svalbard (electronic data available from the European Monitoring and Evaluation Programme at http://www.emep.int/). Data points bounded between broken lines in each graph show agreement within a factor of two. The aerosol measurements were performed to either bulk or size-resolved (submicron and supermicron) aerosol samples taken on a daily to weekly basis depending on the stations. The simulated size-segregated sulfate and sea-salt aerosol concentrations are averaged in time and integrated over size bins so as to match sampling intervals and methods for corresponding field data. The mass ratio of sodium to dry sea salt is assumed to be 30.77% (Gong et al., 2003).

Zeppelin, Svalbard where the model simulates 3 to 5 times greater concentrations in a majority of cases. For sodium, more than half of the cases are outside the range of a-factor-of-two agreement, either over-predicted or under-predicted, at the three sites examined here. This is not surprising, particularly because our present model does not include the production mechanisms of sea-salt aerosols via frost flowers abrasion (Rankin et al., 2002) and via blowing snow sublimation (Yang et al., 2008). At Zeppelin, the over-prediction of sea-salt aerosol concentrations is most likely caused by a bias in simulated surface wind speeds leading to large sea-salt production fluxes around the site (see Sect. S1). Fortunately, both the simulated and observed concentrations of sea-salt aerosols are smaller than those of the sulfate aerosols by more than an order of magnitude in most cases, so that the sulfate aerosols, which are simulated reasonably, play a major role in controlling the rates of heterogeneous reactions of inorganic bromine species (Reactions G130-132) in our model runs.

As discussed in Sect. 3.1 of the main paper, the overprediction of sulfate aerosol concentrations at Zeppelin may be partially responsible for unrealistically strong bromine activation simulated around this site. But, considering challenges faced by state-of-the-art aerosol transport models in simulating physical processes such as precipitation scavenging and long-range transport in the Arctic (Korhonen et al., 2008; Shindell et al., 2008), the general capability of our present model is quite satisfactory.

S3 Back-trajectories from Alert, Barrow and Zeppelin

To gain an insight into a possible link between simulated 'BrO clouds' and ODEs at downwind locations, we also looked at back-trajectories starting from three Arctic locations that correspond to Alert, Barrow and Zeppelin.

Fig. S5 shows 5-day backward trajectories from Alert, Barrow and Zeppelin at three pressure levels (950, 900 and 850 hPa) for each day between 15-22 April 2001, generated by the Canadian Meteorological Centre (CMC) trajectory model (Stocki et al., 2005; Sharma et al., 2006; Chan and Vet, 2010). The model uses 3-D wind fields generated by the GEM model during the process of operational weather forecast at CMC.[1] The model resolution and physical parameterizations employed for CMC's weather forecast are somewhat different from those employed for GEM-AQ simulations in this study. Therefore the trajectories obtained are not necessarily consistent with advection in our model runs and should be viewed only as diagnostic information.

[1]D'Amours, R. and Pagé, P., Atmospheric transport models for environmental emergencies, CMC internal document, Canadian Meteorological Centre, Dorval, Quebec, 2001

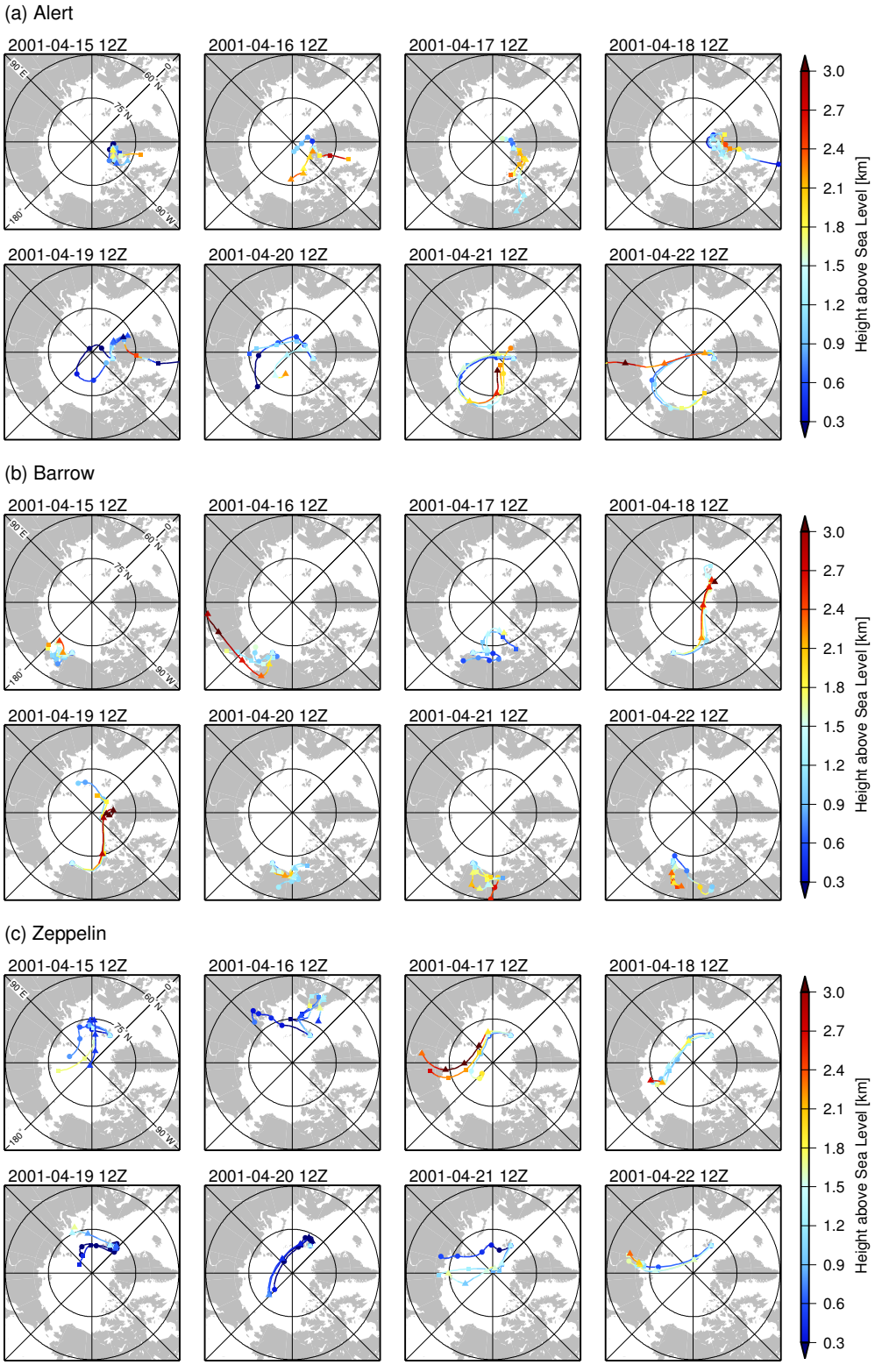

Fig. S5. **(a)** 5-day backward trajectories from Alert starting back at 950, 900 and 850 hPa levels (marked by circles, squares and triangles, respectively, indicating air parcel locations every 24 hours) at 12 UTC for each day between 15-22 April 2001. The height above sea level where air parcel is located is also indicated; **(b)** The same as (a) but backward trajectories from Barrow; and **(c)** The same as (a) but backward trajectories from Zeppelin.

References

Blechschmidt, A.-M.: A 2-year climatology of polar low events over the Nordic Seas from satellite remote sensing, Geophys. Res. Lett., 35, L09 815, doi:10.1029/2008GL033706, 2008.

Bromwich, D. H., Du, Y., and Hines, K. M.: Wintertime surface winds over the Greenland ice sheet, Mon. Wea. Rev., 124, 1941–1947, 1996.

Cassano, J. J., Box, J. E., Bromwich, D. H., Li, L., and Steffen, K.: Evalution of Polar MM5 simulations of Greenland's atmospheric circulation, J. Geophys. Res., 106, 33 867–33 889, 2001.

Chan, E. and Vet, R. J.: Baseline levels and trends of ground level ozone in Canada and the United States, Atmos. Chem. Phys., 10, 8629–8647, 2010.

Croci-Maspoli, M., Schwierz, C., and Davies, H. C.: A multifaceted climatology of atmospheric blocking and its recent linear trend, J. Climate, 20, 633–649, 2007.

Crosby, D. S., L. C. Breaker, L. C., and Gemmill, W. H.: A proposed definition for vector correlation in geophysics: Theory and application, J. Atmos. Oceanic Technol., 10, 355–367, 1993.

Curry, J.: On the formation of continental polar air, J. Atmos. Sci., 40, 2278–2292, 1983.

Curry, J. A. and Ebert, E. E.: Annual Cycle of Radiation Fluxes over the Arctic Ocean: Sensitivity to Cloud Optical Properties, J. Climate, 5, 1267–1280, 1992.

Cuxart, J., Holtslag, A. A. M., Beare, R. J., Bazile, E., Beljaars, A., Cheng, A., Conangla, L., Ek, M., Freedman, F., Hamdi, R., Kerstein, A., Kitagawa, H., Lenderink, G., Lewellen, D., Mailhot, J., Mauritsen, T., Perov, V., Schayes, G., Steeneveld, G.-J., Svensson, G., Taylor, P., Weng, W., Wunsch, S., and Xu, K.-M.: Single-column model intercomparison for a stably stratified atmospheric boundary layer, Boundary-Layer Meteorol., 118, 273–303, 2006.

Environment Canada: Canadian National Atmospheric Chemistry (NAtChem) Database, 2001.

Gong, S. L., Barrie, L. A., Blanchet, J. P., von Salzen, K., Lohmann, U., Lesins, G., Spacek, L., Zhang, L. M., Girard, E., Lin, H., Leaitch, R., Leighton, H., Chylek, P., and Huang, P.: Canadian Aerosol Module: A size-segregated simulation of atmospheric aerosol processes for climate and air quality models 1. Module development, J. Geophys. Res., 108(D1), 4007, doi: 10.1029/2001JD002002, 2003.

Hopper, J. F., Barrie, L. A., Silis, A., Hart, W., Gallant, A. J., and Dryfhout, H.: Ozone and meteorology during the 1994 Polar Sunrise Experiment, J. Geophys. Res., 103, 1481–1492, 1998.

Inoue, J., Liu, J., Pinto, J. O., and Curry, J. A.: Intercomparison of Arctic regional climate models: Modeling clouds and radiation for SHEBA in May 1998, J. Climate, 19, 4167–4178, 2006.

Korhonen, H., Carslaw, K. S., Spracklen, D. V., Ridley, D. A., and Ström, J.: A global model study of processes controlling aerosol size distributions in the Arctic spring and summer, J. Geophys. Res., 113, D08 211, doi:10.1029/2007JD009114, 2008.

Mailhot, J., Tremblay, A., Bélair, S., Gultepe, I., and Isaac, G. A.: Mesoscale simulation of surface fluxes and boundary layer clouds associated with a Beaufort Sea polynya, J. Geophys. Res., 107(C10), 8031, doi:10.1029/2000JC000429, 2002.

Maxwell, J. B.: The Climate of the Canadian Arctic Islands and Adjacent Waters, vol. 1, Climatological Series No. 30, Environment Canada, Atmospheric Environment Service, 1980.

Ola, P., Persson, G., and Stone, R.: Evidence of forcing Arctic regional climates by mesoscale processes, in: AMS Symposium on Connections between Mesoscale Processes and Climate Variability, 15-16 January 2007, San Antonio, TX, American Meteorological Society, URL http://ams.confex.com/ams/87ANNUAL/techprogram/paper_119015.htm, 2007.

Pelly, J. L. and Hoskins, B. J.: A new perspective on blocking, J. Atmos. Sci., 60, 743–755, 2003.

Quinn, P. K., Shaw, G., Andrews, E., Dutton, E. G., Ruoho-Airola, T., and Gong, S. L.: Arctic haze: current trends and knowledge gaps, Tellus, 59B, 99–114, 2007.

Rankin, A. M., Wolff, E. W., and Martin, S.: Frost flowers: Implications for tropospheric chemistry and ice core interpretation, J. Geophys. Res., 107(D23), 4683, doi:10.1029/2002JD002492, 2002.

Rasmussen, E. A. and Turner, J.: Polar Lows: Mesoscale Weather Systems in the Polar Regions, Cambridge Univ. Press, Cambridge, UK, 2003.

Serreze, M. C. and Barry, R. G.: Synoptic activity in the Arctic basin, 1979-85, J. Climate, 1, 1276–1295, 1988.

Sharma, S., Andrews, E., Barrie, L. A., Ogren, J. A., and Lavoué, D.: Variations and sources of the equivalent black carbon in the high Arctic revealed by long-term observations at Alert and Barrow: 1989-2003, J. Geophys. Res., 111, D14 208, doi: 10.1029/2005JD006581, 2006.

Shindell, D. T., Chin, M., Dentener, F., Doherty, R. M., Faluvegi, G., Fiore, A. M., Hess, P., Koch, D. M., MacKenzie, I. A., Sanderson, M. G., Schultz, M. G., Schulz, M., Stevenson, D. S., Teich, H., Textor, C., Wild, O., Bergmann, D. J., Bey, I., Bian, H., Cuvelier, C., Duncan, B. N., Folberth, G., Horowitz, L. W., Jonson, J., Kaminski, J. W., Marmer, E., Park, R., Pringle, K. J., Schroeder, S., Szopa, S., Takemura, T., Zeng, G., Keating, T. J., and Zuber, A.: A multi-model assessment of pollution transport to the Arctic, Atmos. Chem. Phys., 8, 5353–5372, 2008.

Stocki, T., Blanchard, X., D'Amours, R., Ungar, R., Fontaine, J., Sohier, M., Bean, M., Taffary, T., Racine, J., Tracy, B., Brachet, G., Jean, M., and Meyerhof, D.: Automated radioxenon monitoring for the comprehensive nuclear-test-ban treaty in two distinctive locations: Ottawa and Tahiti, J. Environ. Radioactivity, 80, 305–326, 2005.

Takizawa, T. and Kikuchi, T.: J-CAD drifting buoy data, Arctic Ocean, 2000-2002, National Snow and Ice Data Center, Boulder, Colorado, URL http://nsidc.org/data/arcss126.html, digital media, 2004.

Tyrlis, E. and Hoskins, B. J.: Aspects of a Northern Hemisphere atmospheric blocking climatology, J. Atmos. Sci., 65, 1638–1652, 2008a.

Tyrlis, E. and Hoskins, B. J.: The morphology of Northern Hemisphere blocking, J. Atmos. Sci., 65, 1653–1665, 2008b.

Walsh, J. E. and Chapman, W. L.: Arctic Cloud–Radiation–Temperature Associations in Observational Data and Atmospheric Reanalyses, J. Climate, 11, 3030–3045, 1998.

Yang, X., Pyle, J. A., and Cox, R. A.: Sea salt aerosol production and bromine release: Role of snow on sea ice, Geophys. Res. Lett., 35, L16 815, doi:10.1029/2008GL034536, 2008.